



Open Access : : ISSN 1847-9286

<https://pub.iapchem.org/ojs/index.php/JESE>

Original scientific paper

Ni-MoO₂ cathodes for hydrogen evolution in alkaline solutions. Effect of the conditions of their electrodeposition

GVOZDEN TASIĆ, BORKA JOVIĆ*, UROŠ LAČNJEVAC*, NEDELJKO KRSTAJIĆ** and VLADIMIR JOVIĆ*✉

University of Belgrade, Vinča Institute, Department of Physical Chemistry, 11001 Belgrade, P.O. Box 522, Serbia

*Institute for Multidisciplinary Research University of Belgrade, 11030 Belgrade, P.O. Box 33, Serbia

**Faculty of Technology and Metallurgy University of Belgrade, 11000 Belgrade, Karnegijeva 4, Serbia

✉ Corresponding Author: E-mail: E-mail: vladajovic@imsi.rs; Tel.: +381-11-3303-688; Fax: +381-11-3055-289

Received: August 29, 2012; Revised: November 2, 2012; Published: December 4, 2012

Abstract

The electrodeposition of Ni-MoO₂ composite coatings is a specific process taking place under defined hydrodynamic conditions. In this work the influence of hydrodynamics, current density, and MoO₂ concentration on the electrodeposition of Ni-MoO₂ coatings from a suspension of MoO₂ particles in a Watt's type bath were investigated by comparison of their polarization characteristics for the hydrogen evolution reaction (HER) in 1 M NaOH at room temperature. It was shown that electrolyte and air flow rates influence the process of coating electrodeposition at low concentrations of MoO₂. With increases in MoO₂ concentration the current density became the main parameter influencing the coatings' properties. The best coating, with the lowest over-voltage for the HER, was obtained from the suspension containing 3 g dm⁻³ of MoO₂ particles. The over-voltage of this coating was 57 mV lower for the HER at $j = -0.3 \text{ A cm}^{-2}$ (the current density used in industrial applications) than that for the commercial De Nora's Ni + RuO₂ electrode.

Keywords

Ni-MoO₂; composite coatings; electrodeposition; HER; morphology.

Introduction

One of about 90 hydrogen production routes [1] is alkaline water electrolysis [2]. It is a well-established process that is technologically very simple and produces very clean gases, but it is also energy-inefficient, slow, and expensive. One of the ways to increase the energy efficiency of electrolyzers is by developing advanced electrocatalytic materials in order to reduce the electrode over-voltage. In conventional water electrolysis, the cathode is usually made of stainless steel or nickel-based materials (Raney Ni), and operates in 6–9 M KOH solution in a temperature range of 60–90 °C. The overall energy efficiency of electrolysis is related to the hydrogen evolution reaction (HER). In chlor-alkaline electrolysis, HER, as the cathodic reaction in 32 wt.% NaOH at 90 °C, is also responsible for the energy efficiency of electrolyzers [3]. Hence, for industrial application, advanced electrocatalytic materials for HER are of great importance to increase energy efficiency. Since porous Ni (Raney Ni) electrodes showed extensive deactivation during electrolysis, several approaches to design and produce new electrocatalytic cathode materials have been presented in the past [4–20]. One of these approaches is based on the Brewer intermetallic bonding theory, which predicts a synergetic activation effect whenever metals of the left half of the d-series are alloyed with metals of the right half of the d-series [4–10]. Accordingly, an increase in electrocatalytic activity has been widely observed for such materials: Ti–Ni [11], Pt–Mo [12], Ni–Mo [9], Ni–Co–LaNi₅ [13], Ni–RuO₂ [14], and Ni–transition metals (Fe, Mo, W) [15]).

Recently, particular attention has been given to the replacement of expensive Ni + RuO₂ [14] composite coating with coatings obtained by the electrodeposition of Ni with molybdenum oxide species [16–20]. It was shown that Ni–MoO₃ [16,20] composite coatings, electrodeposited from a suspension containing different concentrations of MoO₃ particles in a Watt's type bath, possess good catalytic activity, but their properties during the "service life" test were not good enough for application in industrial electrolysis [18]. On the other hand, Ni–MoO₂ composite coatings electrodeposited from a suspension containing 3 g dm⁻³ MoO₂ particles in a solution of 0.2 M NiCl₂ + 2 M NH₄Cl were found to be a promising replacement [17,18] for commercial Ni + RuO₂ coating obtained by a similar electrodeposition procedure.

Taking into account that the commercial Ni + RuO₂ cathodes were electrodeposited by incorporation of RuO₂ particles in an Ni matrix, in this work an attempt was made to produce Ni–MoO₂ composite coatings from a suspension of MoO₂ particles in a Watt's type bath under different conditions (different concentrations of MoO₂ particles, different current densities, and different hydrodynamic conditions) and to compare their polarization characteristics for HER in 1 M NaOH with that for the commercial Ni + RuO₂ coating. In this way most of the possibilities of obtaining Ni–Mo–oxide coatings by electrochemical deposition would be fulfilled.

Experimental

Electrodeposition of the Ni–MoO₂ composite coatings

The MoO₂ powder was synthesized by a rheological phase reaction route [18]. The average size of MoO₂ powder particles, determined with a Brookhaven Instruments light-scattering system equipped with a BI-200SM goniometer, a BI-9000AT correlator, a temperature controller, and a Coherent INNOVA 70C argon-ion laser, amounted to about 200 nm. Dynamic light scattering measurements were performed using 135 mW laser excitation at a wavelength of 514.5 nm and a detection angle of 90°. All samples were electrodeposited onto Ni 40 mesh from the suspension of MoO₂ powder particles (1–3 g dm⁻³) in a Watt's type electrolyte containing 210 g dm⁻³ NiSO₄ × 7H₂O, 60 g

dm^{-3} $\text{NiCl}_2 \times 6\text{H}_2\text{O}$, 60 g dm^{-3} Na_2SO_4 , and 30 g dm^{-3} H_3BO_3 at $\text{pH} = 3.8$ and $t = 50 \text{ }^\circ\text{C}$ in the pilot plant cell (Fig. 1a,b,c). The electrolyte was circulated with the pump, while the flow rate was measured with the flow meter (Fig. 1a). Additional mixing of the electrolyte was provided by the air flow (measured with the flow meter, Fig. 1b) through two pipes with small openings facing the bottom of the cell in order to remove eventually precipitated molybdenum oxide particles from the bottom of the cell and to force particles to float and circulate with the electrolyte (Fig. 1b,c). The temperature of the electrolyte was kept constant by the thermocouple, heater, and control unit (as shown in Fig. 1a). The Ni 40 mesh cathode (dimensions: $5 \times 6 \text{ cm}^2$) was connected to a Ni holder (frame, Fig. 1d) and placed between two Ni anode plates ($18 \times 22 \text{ cm}$, Fig. 1b). A homemade power supply, with a ripple smaller than 1%, was used to apply the required current/voltage [16,17].

All Ni 40 mesh substrates were first cathodically degreased in a solution of 30 g dm^{-3} NaOH , 30 g dm^{-3} Na_2CO_3 , and 40 g dm^{-3} $\text{Na}_3\text{PO}_4 \times 12\text{H}_2\text{O}$ for 5 min at $j = -100 \text{ mA cm}^{-2}$ and $t = 60 \text{ }^\circ\text{C}$. Neutralization was performed in a solution of 20 g dm^{-3} H_2SO_4 for 5 min. The Ni 40 meshes were then shortly etched in a 1:3 mixture of $\text{H}_2\text{O}:\text{HNO}_3$ and washed with distilled water before the electrodeposition of the Ni– MoO_2 composite coatings.

HER investigations

All experiments were carried out in 1 M NaOH at room temperature in a three-compartment electrochemical cell with two Pt mesh counter electrodes placed parallel (in separate compartments) to the working electrode and a saturated calomel electrode (SCE) as the reference electrode, connected to the working electrode (in the central compartment) by means of a Luggin capillary. The solution of 1 M NaOH was made from extra pure UV water (Smart2PureUV, TKA) and p.a. chemicals.

All experiments were performed with the potentiostat Reference 600 and PHE 200 or DC 105 Software (Gamry Instruments).

Polarization curve measurements

Electrodes were first submitted to hydrogen evolution at a constant current density of $j = -0.3 \text{ A cm}^{-2}$ for 800 s (step 1), followed by HER at a constant potential at which the cathodic current density for HER was higher than -0.3 A cm^{-2} (step 2) for 800 s. After this pre-electrolysis, polarization curves were recorded by sweeping the potential at 1 mV s^{-1} from the potential applied in step 2 to the potential value of -1.10 V and recording the current density. The potential values were corrected for the IR drop by the current interrupt technique (DC 105).

SEM and EDS analysis of the Ni– MoO_2 composite coatings

The appearance of the surface and the chemical composition of the coatings were investigated by SEM (VEGA TS 5130 MM, Tescan) equipped with an energy-dispersive x-ray spectroscope (EDS; INCAPentaFET-x3, Oxford Instruments).

Results and Discussion

Electrodeposition of Ni– MoO_2 samples

Samples 1–12 were deposited with a charge of 60 C cm^{-2} , while samples 13–21 were deposited with a charge of 120 C cm^{-2} . The conditions of electrodeposition are given in Table 1, while

corresponding values of potential taken from the polarization curves for HER in 1 M NaOH at $j = -0.3 \text{ A cm}^{-2}$ are presented in the last column of Table 1.

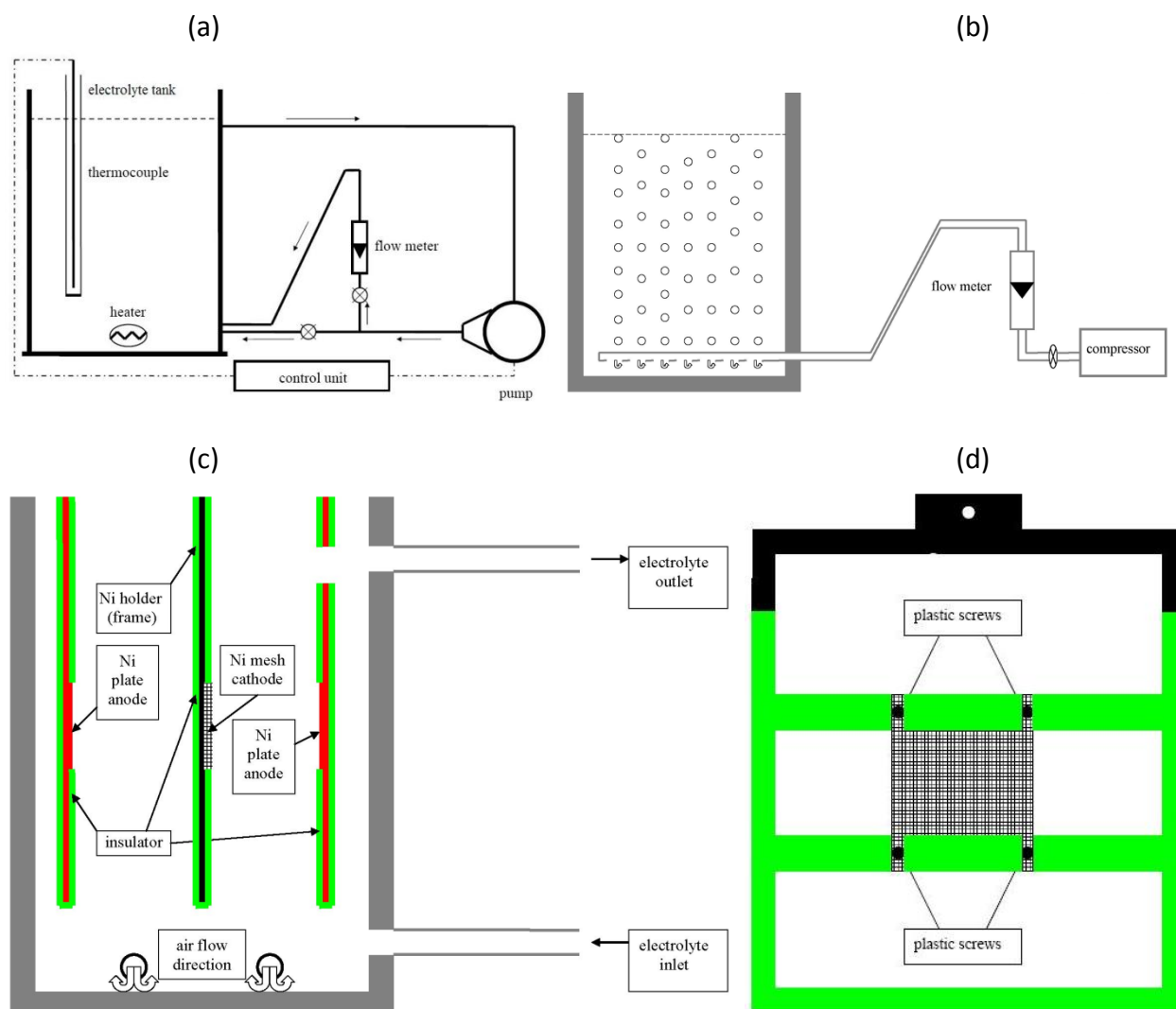


Figure 1. (a) Schematic presentation of the system for electrodeposition of coatings. (b) System for additional mixing of electrolyte with air bubbling through two pipes on the bottom of the tank. (c) Position of anodes and cathode. (d) Position of the mesh cathode on the Ni frame.

Before the addition of MoO₂ powder particles to the electrolyte, electrodeposition of several pure Ni samples in a Watt's type bath was performed at $j = -50 \text{ mA cm}^{-2}$ with different electrolyte and air flow rates. In all cases good quality deposits were obtained with a high current efficiency (> 85 %). When the first amount of MoO₂ powder particles of 1 g dm^{-3} was added to the electrolyte, electrolyte was cycled at the highest rate of $20 \text{ dm}^3 \text{ min}^{-1}$ (with the pump, Fig. 1a) and mixed with the highest air flow of $20 \text{ dm}^3 \text{ min}^{-1}$ (using a compressor, Fig. 1b) for several hours. Electrodeposition of Ni-MoO₂ composite coating started after 24 h of electrolyte aging (following experience from our previous work [17]).

The electrolyte flow rates were set at two values, 10 and $20 \text{ dm}^3 \text{ min}^{-1}$, while the air flow rates were 1, 5, 10, and $20 \text{ dm}^3 \text{ min}^{-1}$. Three values of the deposition current densities (j_{dep}) were used: -25 mA cm^{-2} , -50 mA cm^{-2} , and -100 mA cm^{-2} .

Polarization curves for the best samples

Four samples were deposited in the suspension containing $1 \text{ g dm}^{-3} \text{ MoO}_2$. Their polarization curves for HER were similar, with the best one being that for sample 4. All samples possessed lower over-voltage for HER than Ni 40 mesh with about $50 \text{ }\mu\text{m}$ of pure Ni deposited from the Watt's type bath (Ni). The best sample (4) was deposited at the highest current density and flow rates of electrolyte and air (see Table 1). Nine samples were deposited in the suspension containing $2 \text{ g dm}^{-3} \text{ MoO}_2$. The best polarization characteristics were recorded for sample 13 and the worst ones for sample 11, while all others were placed between these two. Eight samples were deposited in the suspension containing $3 \text{ g dm}^{-3} \text{ MoO}_2$. The best polarization characteristics were recorded for sample 19, while all others were placed close to the best one. The best polarization characteristics for samples deposited from all three suspensions are presented in Fig. 2, together with polarization characteristics for the deposited Ni coating (Ni) and commercial De Nora's Ni + RuO₂ (DN) coating.

Table 1. Conditions for electrodeposition of Ni-MoO₂ coatings.

Sample	MoO ₂ g dm ⁻³	-j _{dep} mA cm ⁻²	Electrolyte flow rate, dm ³ min ⁻¹	Air flow rate, dm ³ min ⁻¹	E _(-0.3 A cm⁻²) V
1	1	25	10	1	-1.480
2		25	10	5	-1.446
3		50	10	1	-1.437
4		50	10	5	-1.437
5	2	25	10	1	-1.466
6		25	10	5	-1.469
7		50	10	5	-1.400
8		50	10	1	-1.430
9		50	10	10	-1.400
10		50	10	20	-1.434
11		50	20	10	-1.463
12		50	20	5	-1.420
13	50	20	5	-1.393	
14	3	50	20	5	-1.343
15		50	20	10	-1.324
16		25	20	10	-1.358
17		100	20	10	-1.309
18		100	20	10	-1.267
19		50	20	10	-1.270
20		50	10	5	-1.284
21		25	10	5	-1.295
DN					

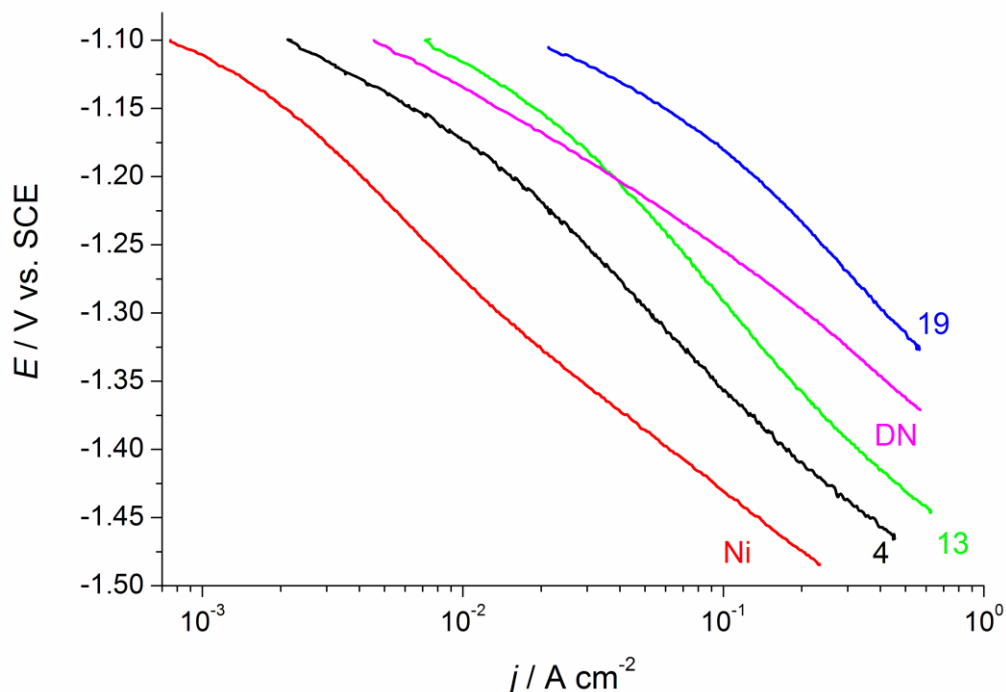


Figure 2. The best polarization curves recorded in 1 M NaOH at room temperature for samples deposited in the suspensions containing 1 g dm⁻³ MoO₂ (sample 4), 2 g dm⁻³ MoO₂ (sample 13), and 3 g dm⁻³ MoO₂ (sample 19). Polarization curves for deposited Ni (Ni) and commercial De Nora’s Ni + RuO₂ electrode (DN).

Morphology of electrodeposited samples

The typical morphology of the electrodeposited samples is presented in Fig. 3a. Two different types of deposits could be clearly seen: a bright, compact deposit, rich in Ni, around the position where the Ni wires crossed, and a dark deposit characterized by a large number of cracks, rich in Mo, located on the rest of the surfaces of the Ni wires. The Ni-rich and Mo-rich parts of the surfaces were analysed by EDS, as shown in Fig. 3b. The results of the EDS analysis are presented in Table 2.

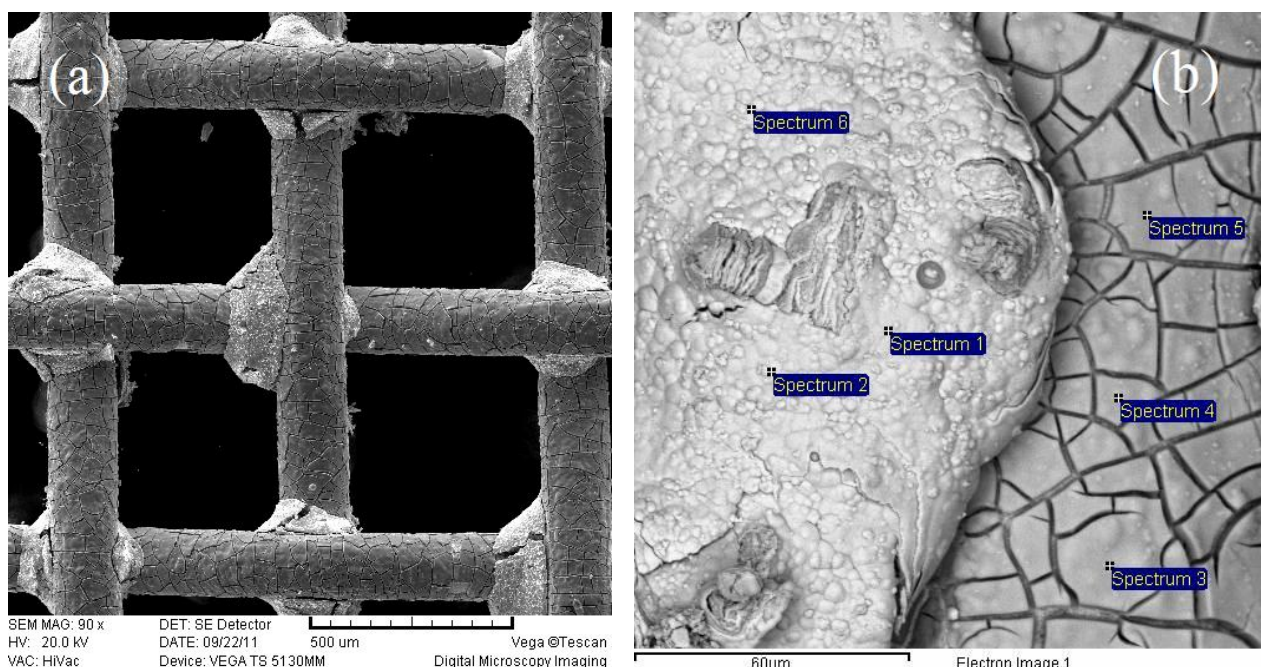


Figure 3. (a) SEM of the surface of a typical deposit; (b) EDS analysis of Ni-rich and Mo-rich surfaces.

Table 2. Chemical compositions of sample surface presented in Fig. 3b.

Spectrum No.	O content, at. %	Ni content, at. %	Mo content, at. %	Average values		
				O content, at. %	Ni content, at. %	Mo content, at. %
1	36.45	50.57	12.98			
2	30.57	58.24	11.19	37	51	12
6	45.43	44.31	10.26			
3	75.14	4.08	20.77			
4	76.04	4.74	19.22	76	5	19
5	76.10	5.13	18.77			

As can be seen, spectra 1, 2, and 6 correspond to the Ni-rich surface, while spectra 3, 4, and 5 correspond to the Mo-rich surface. Similar morphologies and compositions were obtained for samples electrodeposited from ammoniacal NiCl₂ solution [17–19], except that a larger part of the surface of the Ni–MoO₂ composite coatings obtained in our previous work [17–19] was richer in Ni, while a smaller part contained a high percentage of Mo.

In chlor-alkali electrolysis the efficiency of the cathodes results from the combination of a certain activity and stability at the high current densities (3–6 kA m⁻²) used in technological applications. One of the main reasons for the loss of activity and stability of cathodes during long-term operation is the so-called polarity inversion of the electrodes which takes place during the replacement of old electrodes of an electrolyser with new ones in zero-gap cells. During this operation anodes and cathodes are short-circuited, causing a reverse current flow which may damage the cathodes and negatively affect their activity for HER [3]. Manufacturers can predict how often this operation should be performed during a certain period of time and, in accordance with that, design appropriate accelerated “service-life” tests for cathodes. The service-life test of cathode materials that are promising for use in industrial chlor-alkali electrolysis is the subject of only two papers in the literature [18,21]. The procedure for testing the service life is based on a sequence of galvanostatic polarizations in the HER range and cyclic voltammeteries (CVs) in a wide potential range, inducing hydrogen evolution at its negative limit and oxygen evolution at its positive limit (reproducing the conditions of polarity inversion [18,21]). As shown in our previous paper [18] the main reason for the loss of activity of Ni–MoO₂ composite coatings is the dissolution of Mo-rich parts of the coating during the anodic polarization. Although the morphology and composition analysis of Ni–MoO₂ composite coatings obtained in this work indicates the presence of large amount of deposit with Mo-rich parts, their performance during the service-life test will be the subject of our further work.

Conclusions

In this work the influence of hydrodynamics, current density, and MoO₂ concentration on the electrodeposition of Ni–MoO₂ coatings from a suspension of MoO₂ particles in a Watt’s type bath was investigated by comparison of their polarization characteristics for HER in 1 M NaOH at room temperature. It was shown that electrolyte and air flow rates influence the process of coatings electrodeposition at low concentrations of MoO₂, while at higher concentrations of MoO₂ the current density became the main parameter influencing the coatings’ properties. The best coating was obtained from the suspension containing 3 g dm⁻³ of MoO₂ particles. This coating had a 57 mV lower over-voltage for the HER at $j = -0.3 \text{ A cm}^{-2}$ than a commercial De Nora’s Ni + RuO₂ electrode.

Acknowledgements: The authors are indebted to the Ministry of Education and Science of the Republic of Serbia (Project No. 172054) for the financial support of this work as well as to the Department for the Research and Development of De Nora Industries S.p.A. for providing them with the commercial De Nora's cathode for hydrogen evolution in the chlor-alkali plants.

References

- [1] C.J. Winter, J. Nitsch, *Hydrogen as an energy carrier: technologies, systems, economy*, Springer-Verlag, Berlin, New York, 1988
- [2] J.O. Jensen, V. Bandur, N.J. Bjerrum, S.H. Jensen, S. Ebbesen, M. Mogensen, N. Topf, L. Yde, *Pre-investigation of water electrolysis*, Energinet.dk, 2008
- [3] C. Iwakura, M. Tanaka, S. Nakamatsu, H. Noue, M. Matsuoka, N. Furukawa, *Electrochim. Acta* **40** (1995) 977-982
- [4] L. Brewer, in *Alloying*, J.L. Walter, M.R. Jackson, C.T. Sims, Ed(s)., ASM International, New York, USA, 1988, p. 1
- [5] L. Brewer, P.R. Wengert, *Metall. Trans.* **4** (1973) 83-103
- [6] L. Brewer, *Science* **161** (1968) 115-122
- [7] K.A. Gschneider, in *Solid state physics: advances in research and applications*, F. Seitz, D. Tunold, Ed(s)., Academic Press, New York, USA, 1964, p. 275
- [8] M.M. Jakšić, Č.M. Lačnjevac, B.N. Grgur, N.V. Krstajić, *J. New Mat. Electrochem. Systems* **3** (2000) 131-144
- [9] J.M. Jakšić, N.V. Krstajić, B.N. Grgur, M.M. Jakšić, *Int. J. Hydrogen Energ.* **23** (1998) 667-681
- [10] P. Sabatier, *La Catalyse en Chimie Organique*, Librairie Polytechnique, Paris, France, 1913
- [11] N.V. Krstajić, B.N. Grgur, N.S. Mladenović, M.V. Vojnović, M.M. Jakšić, *Electrochim. Acta* **42** (1997) 323-330
- [12] B.N. Grgur, N.M. Marković, P.N. Ross, *J. Phys. Chem. B* **102** (1998) 2494-2501
- [13] G. Wu, N. Li, C.S. Dai, D.R. Zhou, *Mater. Chem. Phys.* **83** (2004) 307-314
- [14] A.C. Tavares, S. Trasatti, *Electrochim. Acta* **45** (2000) 4195-4202
- [15] E. Navarro-Flores, Z. Chong, S. Omanovic, *J. Mol. Catal. A* **226** (2005) 179-197
- [16] N.V. Krstajić, Lj. Gajić-Krstajić, U. Lačnjevac, B.M. Jović, S. Mora, V.D. Jović, *Int. J. Hydrogen Energ.* **36** (2011) 6441-6449
- [17] N.V. Krstajić, Lj. Gajić-Krstajić, U. Lačnjevac, B.M. Jović, S. Mora, V.D. Jović, *Int. J. Hydrogen Energ.* **36** (2011) 6450-6461
- [18] V.D. Jović, U. Lačnjevac, B.M. Jović, N.V. Krstajić, *Electrochim. Acta* **63** (2012) 124-130
- [19] U.Č. Lačnjevac, B.M. Jović, V.D. Jović, N.V. Krstajić, *J. Electroanal. Chem.* **677-680** (2012) 31-40
- [20] Borka M. Jović, Uroš Lačnjevac, Vladimir D. Jović, Ljiljana Gajic-Krstajić, Nedeljko V. Krstajić, *J. Serb. Chem. Soc.*, **77** (2012) 211-224
- [21] A.L. Antozzi, C. Bargioni, L. Iacopetti, M. Musiani, L. Vazquez-Gomez, *Electrochim. Acta* **53** (2008) 7410-7416